Indian Journal of Chemistry
Vol. 56A, November 2017, pp. 1132-1142

Effect of [NaBr] on the rate of intramolecular base-assisted piperidinolysis of ionized phenyl salicylate in the presence of double-tail cationic surfactant aggregates: DDABr/NaBr/H_2O nanoparticles catalysis

N A Razak, I I Fagge & M N Khan

Department of Chemistry, Faculty of Science, University of Malaya, 50603 Kuala Lumpur, Malaysia

Email: iifagge@gmail.com (IIF)/ niyaz@um.edu.my (MNK)

Received 24 August 2017; revised and accepted 30 October 2017

The nucleophilic reactions of piperidine with ionized phenyl salicylate (PSa^-) reveal a nonlinear decrease with the increase in concentration of didodecyldimethylammonium bromide (DDABr) micelles (D_n) at 35 °C and in the absence as well as presence of constant [NaBr]. The plots of pseudo-first-order rate constants (k_{obs}) versus [D_n]) have been explained quantitatively in terms of pseudophase micellar model. Such a data treatment gives DDABr micellar binding constant (K_S) of PSa^-. The effects of [NaBr] upon K_S is explained with an empirical relationship which provides an empirical constant ($K_{Br/S}$ where S = PSa^-). The magnitude of $K_{Br/S}$ is the measure of the ability of ion Br^- to expel the co-ion PSa^- from the cationic micellar pseudophase to the bulk aqueous phase. The origin of the large catalytic effect of DDABr/NaBr/H_2O nanoparticles on the rate of piperidinolysis of PSa^- is described in terms of plausible physicochemical causes.

Keywords: Kinetics, Pseudophase micellar model, Counterion binding-micellar growth, Phenyl salicylate, Piperidine, Cationic micelles, Didodecyldimethylammonium bromide

Kinetic studies on the rates of especially micellar-catalyzed organic reactions led to the emergence of pseudophase micellar (PM) model which provides indirect evidence for micellar structural details in terms of interfacial polarity[1-3], counterion-induced micellar structural transition from spherical-to-wormlike micelles-to-vesicles[4-7], and determination of micellar binding constants of solubilizates[8,9]. Effects of the concentrations of nonreactive NaBr on kinetically determined cetyltrimethylammonium bromide (CTABr) micellar binding constants (K_S) of ionized phenyl salicylate (PSa^-) were rationalized by the empirical equation (Eq. (1))

$$K_S = K_S^0/\left(1+K_{Br/S}[NaBr]\right) \quad \ldots (1)$$

where $K_S^0 = K_S$ at [NaBr] = 0 and $K_{Br/S}$ represents an empirical constant whose magnitude is the measure of the ability of Br^- to expel S^- from the cationic micellar pseudophase to the bulk aqueous phase[10]. The kinetic probe reaction, used to determine the values of K_S at different [NaBr], is the nucleophilic substitution reaction between piperidine (Pip) and PSa^-. It can be easily shown that a kinetic equation derived from a reaction scheme for CTABr micellar-catalyzed reaction of Pip with PSa^- in terms of PM model and Eq. (1) can lead to Eq. (2) at a constant temperature and $[CTABr]_T$ (total concentration of CTABr)

$$k_{obs} = \frac{k_0 + \theta K^{Br/S}[NaBr]}{1 + K^{Br/S}[NaBr]} \quad \ldots (2)$$

where θ and $K^{Br/S}$ are the empirical constants, $k_0 = k_{obs}$ at [NaBr] = 0 and [CTABr] ≠ 0[11]. Eq. (2) has been found to be valid for different types of counterionic salts (MX) with replacement of $K^{Br/S}$ and NaBr by $K^{X/S}$ and MX respectively[11]. The validity of Eq. (1) or Eq. (2) requires that the structure of aqueous CTABr/MX/H_2O aggregates should remain unchanged within [MX] range covered in the study because the values of $K_{X/S}$ or $K^{X/S}$ for different X^- vary in the order: $K_{X/S}$ or $K^{X/S}$ (for spherical micelles, SM) < $K_{X/S}$ or $K^{X/S}$ (for wormlike micelles, WM) << $K_{X/S}$ or $K^{X/S}$ (for vesicles, Vs)[11,12]. Thus, a break in the plot of K_S versus [MX] or k_{obs} versus [MX] (provided k_{obs} values are independent of [MX] at $[CTABr]_T = 0$) is an evidence for the aqueous cationic surfactant aggregate structural transition [4,12,13].

As described in the semiempirical kinetic (SEK) method, the value of $K^{X/S}$ is a function of $K_{X/S}$, K_S^0 and $[CTABr]_T$[11]. The values of $K_{Br/S}$ (obtained from Eq. (1)), as well as θ and $K_{X/S}$ (obtained from Eq. (2))

can give the value of $R_X^{Br} = K_X/K_{Br}$ where K_X and K_{Br} represent CTABr micellar binding constant in the presence of spherical or nonspherical micelles and spherical micelles respectively[11]. It is noteworthy that SEK method is the only method that gives the values of R_X^{Br} or K_X^{Br} (conventional ion exchange constant) for X representing both hydrophilic and moderately hydrophobic counterions. Almost all other physicochemical methods give the values of only K_X^{Br} and most of these methods give reliable values of K_X^{Br} when X represents hydrophilic counterions[14-16]. Recent studies, related to the effects of counterions on ionic surfactant aggregate growth, reveal that moderately hydrophobic counterions (such as benzoate and substituted benzoates) are industrially more important than hydrophilic counterions[17].

Effects of the concentrations of dialkyl chain cationic surfactants on such surfactant aggregate structural transitions have been extensively studied[18-22]. However, studies on the kinetics and mechanism of didodecyldimethylammonium bromide (DDABr) micellar-catalyzed reactions are only a few[23,24]. Some of these studies on DDABr/H_2O system show the aqueous DDABr aggregate structural transitions as: globular prolate micelles (WM)-very small vesicles (SV_S)-large multilamellar vesicles (MLV)[18]. However, detailed kinetic studies[23,24], carried out on DDABr-catalyzed cleavage of 6-nitrobenzisoxazole-3-carboxylate, assert the presence of premicellar aggregates[23] and ammonium bilayer membranes[24] under essentially similar experimental kinetic conditions. As noted earlier in the text, in view of reported studies[11,12,25], the value of $K_{Br/S}$ should vary in the order: $K_{Br/S}$ (in SM) < $K_{Br/S}$ (in WM) << $K_{Br/S}$ (in Vs). The value of $K_{Br/S}$, obtained in the presence of aqueous cationic CTABr spherical micelles is 25 M^{-1} at 35 °C for S = PSa^-[10]. The present study was carried out with the aim to determine the values $K_{Br/S}$ (for S = PSa^-) in the presence of aqueous cationic DDABr aggregates at 35 °C and to compare these values with $K_{Br/S}$ (= 25 M^{-1}) obtained in the presence of CTABr spherical micelles.

Materials and Methods

Phenyl salicylate (PSaH, Fluka) with a purity of ≥98% and didodecyldimethylammonium bromide (DDABr, Aldrich) with a purity of 98% were used without further purification. All other chemicals were also of reagent grade and were from Merck. The stock solutions of PSaH (10 m*M*) were prepared in acetonitrile. The stock solutions of DDABr (1.0 m*M*) were prepared in 1 L volumetric flask by the use of deionized water (Merck Millipore). Aqueous stock solution was gently shaken to dissolve DDABr completely. Clear and transparent stock solution was then left for nearly two weeks at ambient temperature. This stock solution was used to prepare other stock solutions of lower concentrations by dilution.

Kinetic measurements

Ionized phenyl salicylate (PSa^-) absorbs strongly while hydrolysis and piperidinolysis products of PSa^- absorb weakly at 370 nm and 35 °C in both the absence and presence of DDABr aggregates. In a typical kinetic run, the reaction mixture (4.9 mL) containing all the reaction ingredients except PSaH was temperature equilibrated at 35 °C for about 10 min. The reaction was then started by adding 0.1 mL of PSaH to the temperature equilibrated reaction mixture (4.9 mL). Nearly 2.5 mL of the reaction mixture was quickly transferred to 3 mL quartz cuvette which was kept in the thermostat cell holder of the UV-visible spectrophotometer. The progress of the reaction was monitored by recording the decrease in absorbance (A_{ob}) as a function of reaction time (t) at 370 nm. All the kinetic runs were carried out until 5–10 half-lives. The observed data (A_{ob} *vs.* *t*) were found to fit well to Eq. (3)

$$A_{ob} = [R_0]\delta_{ap}\exp(-k_{obs}t) + A_\infty \quad \ldots (3)$$

where $[R_0]$ represents initial concentration of PSaH, δ_{ap} is the apparent molar absorptivity of the reaction mixture, k_{obs} is the pseudo-first-order rate constant and $A_\infty = A_{ob}$ at $t = \infty$. Nonlinear least-squares technique was used to calculate k_{obs}, δ_{ap} and A_∞ from Eq. (3) and the observed data fit to Eq. (3) was found to be satisfactory in terms of percent residual errors (%RE = 100 × $(A_{ob\,i} - A_{cald\,i})/A_{ob\,i}$ where $A_{ob\,i}$ and $A_{cald\,i}$ represent observed and least-squares calculated absorbance at the i^{th} reaction time (t_i), as well as standard deviations associated with calculated kinetic parameters k_{obs}, δ_{ap} and A_∞. The details of the data analysis and product characterization are the same as described elsewhere[12].

Results and Discussion

Effect of $[DDABr]_T$ on k_{obs} for the nucleophilic reaction of Pip with PSa^- in absence and presence of NaBr

In order to determine DDABr micellar binding constant (K_S) of PSa^-, several kinetic runs were carried out at 0.2 m*M* PSa^-, 30 mM NaOH, 100 m*M* Pip, 35 °C and within $[DDABr]_T$ (where symbol $[\ ]_T$ represents

total concentration) range 0.0– ≤ 0.8 m*M*. Similar observations were obtained within [NaBr] range 1–100 m*M*. The values of k_{obs} at different $[DDABr]_T$, within its range 0.0– ≤ 0.8 m*M*, are shown in Fig. 1 at a few representative values of [NaBr] and Figs S1 and S2 (Supplementary Data). The calculated values of δ_{ap} at different $[DDABr]_T$ are shown graphically in Fig. 2 at 0.0, 5 and 20 m*M* NaBr and Figs S3 and S4 (Supplementary Data) at 1, 2, 3, 6, 10, 50 and 100 m*M* NaBr. The calculated values of A_∞, at different $[DDABr]_T$ and a constant value of [NaBr], within its range 0.0–100 m*M*, are shown graphically in Figs S5 and S6 (Supplementary Data).

Effect of mixed CH_3CN-H_2O solvents on rate of piperidinolysis of PSa^- in absence of DDABr and NaBr

The values of δ_{ap} at 370 nm were found to be independent of $[CTABr]_T$ at a constant [NaBr] and independent of [NaBr] at $[CTABr]_T = 0$. However, the values of δ_{ap} at different $[DDABr]_T$, in the absence and presence of NaBr, show a nonlinear increase with increasing values of $[DDABr]_T$, within its certain typical ranges (Fig. 2 as well as Figs S3 and S4 (Supplementary Data)). These observations were suspected to be due to medium polarity changes of micellar-catalyzed reactions with increasing values of $[DDABr]_T$. Such micellar effects are generally ascribed as the partial contribution to the total micellar catalytic effects on reaction rate constants[10,26,27]. In order to explore the possibility of the changes in the micellar reaction medium polarity as the cause of the increase in δ_{ap} with the increase in $[DDABr]_T$, a series of kinetic runs was carried out on piperidinolysis of PSa^- within CH_3CN content range 2– ≤ 96% *v/v* in mixed aqueous solvents at a constant [NaOH], 0.1 *M* Pip, 370 nm and 35 °C. The values of k_{obs}, δ_{ap} and A_∞, obtained for several kinetic runs at 5 and 10 m*M* NaOH, are summarized in Table S1 (Supplementary Data). Although the reaction mixtures were weakly cloudy to naked eye at ≥ 90% *v/v* CH_3CN, the observed data fit to the pseudo-first-order kinetic equation was satisfactory as evident from the percent residual errors ($\%RE = 100 \times (A_{ob\,i} - A_{cald\,i})/A_{ob\,i}$ where $A_{ob\,i}$ and $A_{cald\,i}$ represent observed and least-squares calculated absorbance respectively, at the i^{th} reaction time, t_i) listed in Table S2 (Supplementary Data) for two representative kinetic runs.

In view of an earlier study[10], it is evident that protonated piperidine ($PipH^+$) and nonionized phenylsalicylate (PSaH) are not present in the reaction mixtures at a detectable level under the experimental

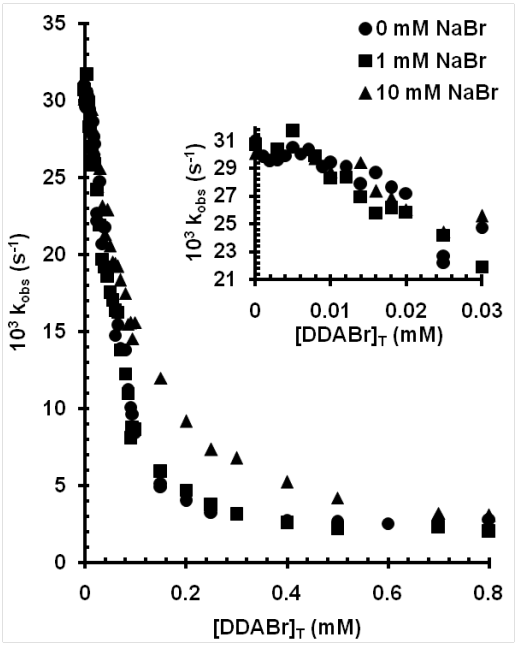

Fig. 1 — Plots showing the dependence of k_{obs} upon $[DDABr]_T$ for piperidinolysis of PSa^- at 0.2 m*M* PSa^-, 0.1 *M* Pip, 0.03 *M* NaOH, 35 °C and different constant values of [NaBr]. [Inset: The plots at magnified scale for the data points at the lowest values of $[DDABr]_T$].

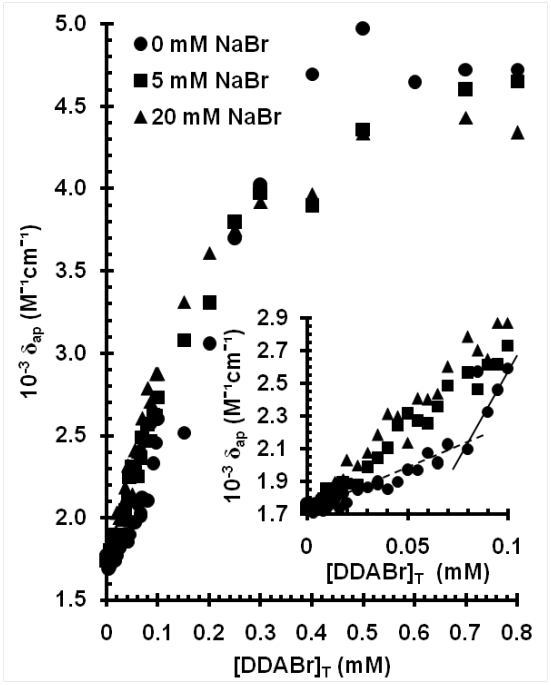

Fig. 2 — Plots showing the dependence of δ_{ap} upon $[DDABr]_T$ f or piperidinolysis of PSa^- at 0.2 m*M* PSa^-, 0.1 *M* Pip, 0.03 *M* NaOH, 35 °C and different constant values of [NaBr]. [Inset: The plots at magnified scale for the data points at the lowest values of $[DDABr]_T$].

conditions of entire kinetic runs of the present study. The rate of hydrolysis is negligible compared to that of piperidinolysis of PSa^- under the experimental conditions of present study[10]. In view of these observations, a brief reaction scheme for the cleavage of PSa^-, under the present experimental conditions, may be expressed by Eq. (4)

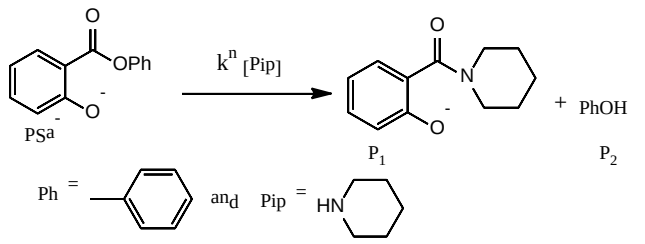

… (4)

where k^n represents nucleophilic second-order rate constant. Effect of cationic micelles of mono chain surfactants on the rate of nucleophilic substitution reaction of Pip with PSa^-, in the absence and presence of an inert salt, have been explained quantitatively in terms of the pseudophase micellar (PM) model of micelles[10,28]. The apparent monotonic decrease of k_{obs} with the increase of $[DDABr]_T$, as exhibited in Fig. 1 as well as Figs S2 and S3 (Supplementary Data), has been attempted to explain in terms of PM model of micelles[29,30]. A brief reaction scheme, in terms of PM model, for piperidinolysis of PSa^- under the present experimental conditions, may be expressed in Scheme 1, where N and D_n represent Pip and DDABr micelles respectively (i.e. $[D_n] = [DDABr]_T$ – CMC with CMC representing critical micelle concentration), and all other symbols have their usual meanings[28]. The observed rate law (rate = $k_{obs}[PSa^-]_T$ where $[PSa^-]_T = [PSa^-_W] + [PSa^-_M]$ and subscripts W and M represent bulk water phase and micellar pseudophase respectively) and Scheme 1 can lead to Eq. (5)

$$k_{obs} = \frac{\left(k^n_W + k^{mr}_M K_N K_S [D_n]\right)[N]_T}{1 + K_S[D_n]} \quad \ldots (5)$$

where $1 >> K_N[D_N]$ under the present experimental conditions[28], $[N]_T = [N_W] + [N_M]$ and $k^{mr}_M = k^n_M / V_M$ where V_M is the micellar molar reaction volume (in M^{-1})[29,30].

The occurrence of ion exchange processes between counterions, in the presence of ionic micelles, appears to be a ubiquitous feature of micellar-mediated reacting systems. Although the possible ion exchange processes in the present reaction system are Br^-/HO^-, HO^-/PSa^- and Br^-/PSa^-, the relatively effective and kinetically detectable ion exchange process is Br^-/PSa^- at a constant $[PSa^-]_T$[10]. The occurrence of ion exchange Br^-/PSa^-, at a constant $[PSa^-]_T$, should change the value of K_S with the increase in $[Br^-]_T$. But the change in K_S with the increase in $[DDABr]_T$ from 0.01 to 0.80 m*M*, at a constant [NaBr], may be considered to be insignificant because of the large difference in hydrophobicity of Br^- and PSa^- and a very small increase in $[Br^-]$.

The values of CMC, at a constant temperature and [NaBr] (within its range 0–100 m*M*), were determined by the kinetic iterative[11] and graphical[31] techniques. The values of CMC, obtained from iterative and graphical techniques, are not appreciably different from each other under a typical reaction condition. The increase in [NaBr] is expected to decrease CMC which is evident within [NaBr] range 0.0–6.0 m*M*. The values of CMC appear to be independent of [NaBr] within its range 10–100 m*M*. Thus, perhaps a more reliable value of CMC at ≥ 10 m*M* NaBr may be the average value of CMC values obtained within [NaBr] range 10–100 m*M*. The value of k_W ($= k^n_W[N]_T$ where $[N]_T = 0.1\ M$), at a constant temperature and [NaBr], was obtained experimentally by carrying out kinetic run(s) at $[D_n] = 0$. The calculated values of CMC and k_W, at different values of [NaBr], are summarized in Table 1. Although the phase behavior of binary system $DDABr/H_2O$ is well established[32], the existence of a CMC and CVC (critical vesicle concentration) in dilute $DDABr/H_2O$ solutions has not been previously demonstrated as clearly as in a few relatively recent reports[18, 19]. The reported values of CMC and CVC at 25 °C are 0.046 m*M*[18], 0.03 m*M*[24], 0.05 m*M*[19], and 0.73 m*M*[18], respectively. The values of CMC and CVC, obtained by the use different techniques, vary in the range 0.018–0.078 m*M* and 0.43–0.88 m*M*, respectively[33]. Graphically determined value of CMC (= 0.011 m*M*, Table 1), obtained at [NaBr] = 0, is significantly lower than the reported values of CMC[18,19,24,33]. This decrease in CMC may be attributed to the presence of 0.2 m*M* PSa^- which is known to decrease CMC of CTABr micelles by nearly 6- to 10- fold[10,11,24,34].

The values of δ_{ap} are independent of $[DDABr]_T$ within its range 0.0–0.01 m*M* and the mean value of δ_{ap} is 1730 ± 27 M^{-1} cm^{-1} in the absence of NaBr. The values of δ_{ap} (Table S1) clearly demonstrate the

Table 1 — Values of the intercept (α) and slope (K_S) of linearized form of Eq. (5) using k_{obs} values obtained at CMC < $[DDABr]_T \leq 0.08$ m*M* and different [NaBr][a]

[NaBr] (m*M*)	10^2 CMC (m*M*)	10^2 CMC[c] (m*M*)	$10^3 k_W$[d] (s^{-1})	α[e]	$10^{-3} K_S$ (M^{-1})	$10^{-3} K_S^{cald}$[f] (M^{-1})	10^2 $[DDABr]_T$ (m*M*)
0.0	1.2	1.2	29.8 ± 0.6[g]	0.78 ± 0.04[g]	17.9 ± 0.9[g]	-	1.2 – 8.0
0.0	1.0	1.0	30.3 ± 0.1	0.81 ± 0.05	19.4 ± 1.1	-	1.0 – 8.0
1.0	0.7	0.6	30.7 ± 0.8	0.91 ± 0.02	16.3 ± 0.6	16.8	1.0 – 6.5
2.0	1.0	0.9	30.4 ± 0.3	0.86 ± 0.02	15.6 ± 0.5	15.6	1.2 – 8.0
3.0	0.7	0.6	30.1 ± 0.3	0.91 ± 0.02	15.7 ± 0.5	14.7	1.0 – 8.0
5.0	0.6	0.5	30.5 ± 0.4	0.94 ± 0.02	13.1 ± 0.4	13.1	1.0 – 8.0
6.0	0.3	0.2	31.6 ± 0.2	0.97 ± 0.02	12.1 ± 0.7	12.4	1.0 – 8.0
10.0	0.8	0.7	29.5 ± 0.6	0.93 ± 0.02	9.64 ± 0.67	10.2	1.6 – 8.0
20.0	0.4	0.4	29.9 ± 0.4	0.97 ± 0.02	7.47 ± 0.40	7.1	1.0 – 8.0
50.0	0.0	0.0	30.3 ± 0.1	1.00 ± 0.01	6.61 ± 0.37	(3.75)[h]	0.7 – 8.0
100.0	0.6	0.5	29.9 ± 0.3	0.96 ± 0.02	8.85 ± 0.43	(2.09)	1.2 – 6.5

[a][PSaH] = 0.2 m*M*, 30 m*M* NaOH, 100 m*M* Pip, 35 °C, λ = 370 nm, aqueous reaction mixture for each kinetic run contains 2% *v/v* CH_3CN.
[b]Values of CMC were obtained from graphical technique.
[c]Values of CMC were calculated from the relationship: α = 1 – CMC K_S with α and K_S values from Table 1.
[d]k_W represents mean value of several k_{obs} obtained within $[DDABr]_T$ range 0– < CMC. [e]α = 1 – CMC K_S.
[f]Calculated from Eq. (1) with $10^{-3} K_S^0 = 18.0\ M^{-1}$ and $K_{Br/S} = 76\ M^{-1}$ as described into the text.
[g]Error limits are standard deviations.
[h]Parenthesized values represent K_S^{cald} calculated from Eq. (1) with $10^{-3}K_S^0 = 18.0\ M^{-1}$ and $K_{Br/S} = 76\ M^{-1}$.

nonlinear increase in δ_{ap}, as exhibited by Fig. 2, is due to decrease in $[H_2O]$ in the micellar environment of micellized PSa^- with the increase in [DDABr] at the constant [NaBr] within its range 0.0–20 m*M*. Such characteristic observations were not obtained in the presence of SM, WM, and Vs produced by CTABr under essentially similar conditions. The values of δ_{ap} remained independent of $[CTABr]_T$ and they revealed the medium polarity of micellized PSa^- equivalent to the polarity of mixed CH_3CN–H_2O solvent containing ~90–92% *v/v* CH_3CN. The plot of Fig. 2 shows distinct aggregate structural transitions at ~0.01 and ~0.08 m*M* DDABr and [NaBr] = 0. These first and second structural transitions may be attributed to the reported CMC and CVC, respectively[18,19,33].

The observed data (k_{obs} *vs.* $[DDABr]_T$), obtained within $[DDABr]_T$ range 0.014–0.080 mM at [NaBr] = 0 (Fig. 1), were used to calculate k_M (= $k_M^{mr} K_N[N]_T$) and K_S from Eq. (5) by the use of nonlinear least-squares technique considering k_W (= $k_W^n[N]_T$) as known parameter. The value of k_W (= (29.9 ± 0.5) × 10^{-3} s^{-1}) was obtained as the mean value of k_{obs} obtained within $[DDABr]_T$ range 0.0–0.01 m*M*. The least-squares calculated values of k_M and K_S are (-1.9 ± 1.6) × 10^{-2} s^{-1} and 8091 ± 3763 M^{-1} respectively with graphically determined value of CMC = 0.012 m*M*. Negative value of k_M, associated with significantly large standard deviation, merely indicates insignificant contribution of $k_M^{mr} K_N K_S[D_n]$ compared with k_W^n and as a consequence $k_W^n >> k_M^{mr} K_N K_S[D_n]$ in Eq. (5) which reduces Eq. (5) to Eq. (6) at $[DDABr]_T \leq 0.08$ m*M*. It is evident from Eq. (6) that a plot of k_W/k_{obs} versus $[DDABr]_T$ should be linear with intercept, α (= 1 – $CMCK_S$) and slope = K_S. The plot of k_W/k_{obs} versus $[DDABr]_T$ appears to be linear at $[DDABr]_T \leq 0.08$ m*M*

$$k_{obs} = k_W / (1 + K_S[D_n]) \quad \ldots (6)$$

as shown in Fig. 3 and Fig. S7 (Supplementary Data). The linear least-squares calculated values of α and K_S are summarized in Table 1. The extent of reliability of the observed data fit to the linear equation: $k_W/k_{obs} = \alpha + K_S[DDABr]_T$, is evident from the percent residual errors, %RE (= 100 × ((k_W/k_{obsi}) – (k_W/k_{caldi}))/(k_W/k_{obsi})) values (where maximum and minimum absolute values of RE are 9.8 and 0.2 % respectively), and standard deviations associated with the calculated values of α and K_S. Similar results were obtained with the repeat set of the kinetic runs under similar conditions where the calculated values of α and K_S are also shown in Table 1.

The value of K_S is expected to be larger in the presence of vesicles than that of WM[19]. The values of rate constants for CTABr micellar-catalyzed reaction of PSa^- with Pip are not sensitive to [NaBr][10]. Plots of

Fig. 3 reveal that the slopes of the linear segments decrease more rapidly in the presence of vesicles compared to WM with increasing [NaBr]. Linear least-squares technique was used to calculate α (= 1 – CMCK_S) and K_S from Eq. (6) by considering k_W as known parameter. The value of k_W was obtained as the mean value of rate constants k_{obs} obtained within 0.0– < CMC. The calculated values of α, K_S and k_W at different [NaBr] (within [NaBr] range 0.0–0.10 *M*) are shown in Table 1.

The break points in the plots of k_W/k_{obs} versus $[DDABr]_T$ could give the values of CVC only at ≤ 0.003 *M* NaBr and such break points virtually disappeared at ≥ 0.005– ≤ 0.020 *M* NaBr (Fig. 3 and Fig. S7, Supplementary Data). The values of CVC at ≥0.005 *M* NaBr were assigned as the specific values of $[DDABr]_T$ where values of δ_{ap} are ~2100–2200 M^{-1} cm^{-1}. The value of δ_{ap}, in the range 2100–2200 M^{-1} cm^{-1}, corresponds to CVC in the plot of δ_{ap} versus $[DDABr]_T$ at [NaBr] = 0 (Fig. 2). These values of CVC are given in Table 2. Since the value of k_W for the kinetic data of vesicle phase is not possible to determine experimentally, the kinetic data of this vesicle phase were tried to fit to Eq. (5) by considering k_W (= $k_W^n[N]_T$), k_M (= $k_M^{mr} K_N[N]_T$) and K_S as three unknown parameters. The nonlinear least-squares calculated values of these unknown parameters at

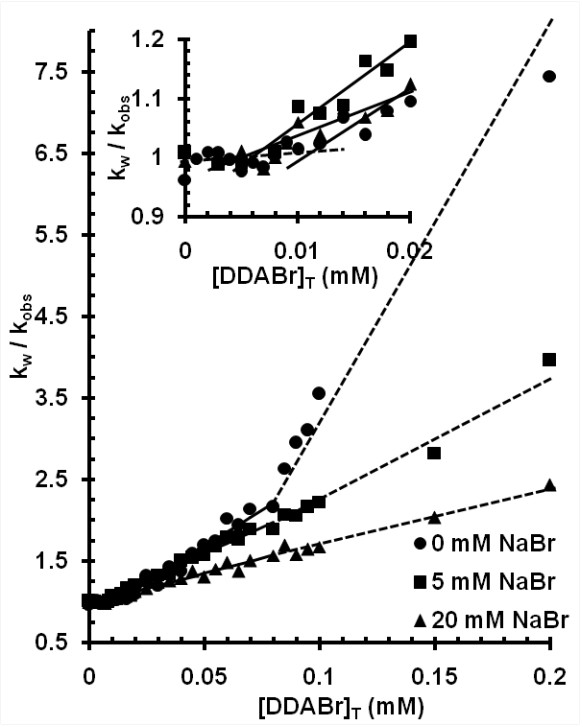

Fig. 3 — Plots showing the dependence of k_W/k_{obs} upon $[DDABr]_T$ for piperidinolysis of PSa^- at 0.2 m*M* PSa^-, 0.1 *M* Pip, 0.03 *M* NaOH, 35 °C and different constant values of [NaBr]. [The solid lines are drawn through the calculated data points using the relationship: $k_W/k_{obs} = \alpha + K_S[DDABr]_T$ with kinetic parameters (α and K_S), listed in Table 1. Inset: The plots at magnified scale for the data points at the lowest values of $[DDABr]_T$].

Table 2 — Values of kinetic parameters, k_W, k_M and K_S, calculated from Eq. (5) using k_{obs} values obtained at CVC < $[DDABr]_T$ ≤ 0.80 m*M* and different values of [NaBr]

[NaBr] (m*M*)	10^2 CVC[a] (m*M*)	$10^3 k_W$ ($10^3 k_{obs}$)[b] (s^{-1})	$10^3 k_M$[c] (s^{-1})	$10^{-3} K_S$ (M^{-1})	$10^{-3} K_S^{cald}$[d] (M^{-1})	10^2[DDABr]$_T$ (m*M*)
0.0	8.0 (8.0)	13.0 ± 0.3[e] (13.8)	1.79 ± 0.14[e]	34.2 ± 3.3[e]		9.0 – 60.0
0.0	8.0 (8.0)	13.8 ± 0.7 (12.8)	1.74 ± 0.21	33.1 ± 6.0	24.4	9.0 – 65.6
1.0	6.6 (7.0)	15.4 ± 0.4 (16.2)	1.21 ± 0.23	25.3 ± 2.9	18.7	8.0 – 80.0
2.0	5.0 (6.6)	16.5 ± 1.0 (18.8)	0.64 ± 0.25	16.1 ± 2.6	15.1	8.5 – 80.0
3.0	8.0 (8.0)	16.5 ± 0.3 (14.3)	0.94 ± 0.28	16.7 ± 1.9	10.9	8.5 – 80.0
5.0	5.0	21.1 ± 2.2 (19.4)	0.32 ± 0.70	11.2 ± 3.2	9.7	9.5 – 80.0
6.0	4.5	20.0 ± 2.0 (20.4)	-0.7 ± 1.0	8.40 ± 2.6	6.5	9.5 – 80.0
10.0	5.5	21.2 ± 1.6	0.0	10.3 ± 1.6	(3.6)[f]	9.5 – 80.0
20.0	4.5	20.4 ± 1.2 (19.5)	-0.1 ± 0.8	8.27 ± 1.8	(1.5)	9.5 – 80.0
50.0	2.5	20.5 ± 0.8	0.0	8.37 ± 0.78	(0.8)	9.5 – 80.0
100.0		23.8 ± 0.4 (22.7)	-0.3 ± 0.4	5.89 ± 0.44		9.5 – 80.0
		24.0 ± 0.3	0.0	6.17 ± 0.18		9.5 – 80.0
		23.0 ± 0.3 (23.7)	-0.7 ± 0.9	2.70 ± 0.25		9.5 – 70.0
		23.3 ± 0.2	0.0	2.93 ± 0.7		9.5 – 80.0
		24.6 ± 1.4 (24.5)	3.96 ± 1.45	4.82 ± 1.44		9.5 – 70.0

[a]Parenthesized values of CVC were obtained from graphical technique.

[b]Parenthesized value represents k_{obs} experimentally obtained at $[DDABr]_T$ = CVC and $k_W = k_W^n[N]_T$ with $[N]_T$ = 0.1 *M*.

[c]$k_M = k_M^{mr} K_N[N]_T$ with $[N]_T$ = 0.1 *M*.

[d]Calculated from Eq. (1) with $10^{-3} K_S^0$ = 35.0 M^{-1} and $K_{Br/S}$ = 437 M^{-1} as described in the text.

[e]Error limits are standard deviations. [f]Parenthesized values represent K_S^{cald} calculated from Eq. (1) with $10^{-3} K_S^0$ = 35.0 M^{-1} and $K_{Br/S}$ = 437 M^{-1}.

different [NaBr] are shown in Table 2. Although the observed data fit to Eq. (5) appears to be satisfactory in terms of residual errors as evident from some representative plots of Fig. 4 where solid lines are drawn through the calculated data points, the values of calculated parameters (k_W, k_M and K_S) may be considered to be less reliable because of uncertainty associated with the values of CVC. Ideally, the value of k_{obs} at CVC should be equal to the corresponding calculated value of k_W using Eq. (5) where $k_W = k_W^n [N]_T$, but these values of k_W and k_{obs} differ in the range of 0.4–15.0% (Table 2).

Some negative calculated values of k_M, listed in Table 2, are physicochemically meaningless. The negative values of k_M with standard deviations of more than 100 % merely indicate that $k_M K_S[D_n] << k_W$ in Eq. (5). Thus, the values of k_W and K_S were also calculated from Eq. (5) with $k_M = 0$. Such calculated values of k_W and K_S are also shown in Table 2. These values of k_W and K_S are not significantly different from the corresponding values of k_W and K_S calculated from Eq. (5) with $k_M \neq 0$.

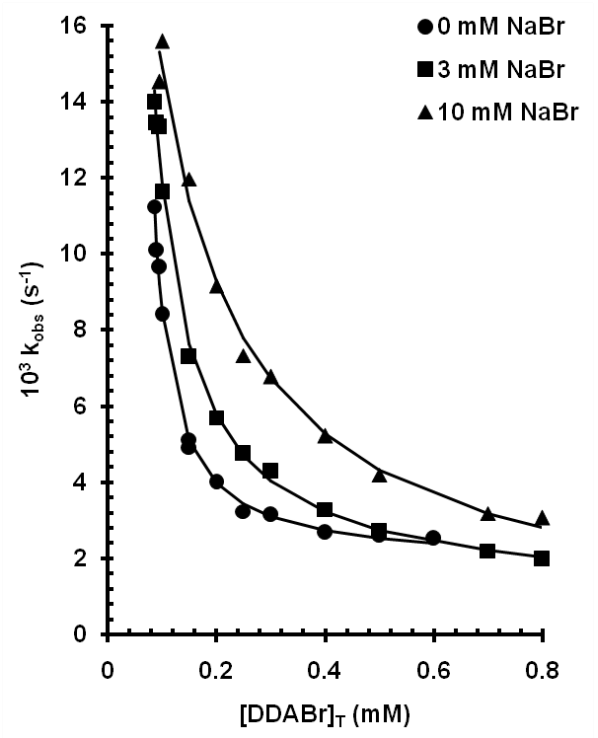

Fig. 4 — Plots showing the dependence of k_{obs} upon $[DDABr]_T$ for piperidinolysis of PSa^- at 0.2 m*M* PSa^-, 0.1 *M* Pip, 0.03 *M* NaOH, 35 °C and different constant values of [NaBr]. [The solid lines are drawn through the calculated data points using Eq. (4) with kinetic parameters (k_M, K_S and k_W), listed in Table 2, at CVC (m*M*) = 0.08 (●), 0.08 (■) and 0.055 (▲)].

A recent study[18] provides experimental evidence for the presence of globular prolate micelles (i.e., WM) at $[DDABr]_T$ > CMC (= 0.046 m*M*) and very small vesicles (SVs) followed by large multilamellar vesicles (MLV) at $[DDABr]_T$ > CVC (= 0.73 m*M* DDABr) in DDABr/D_2O or H_2O system. In view of this report, the structure of DDABr/H_2O aggregates may be considered to be WM and SVs + MLV at > 0.012 and >0.08 m*M* DDABr respectively. Steady-shear rheological measurements on 0.06 m*M* DDABr/H_2O and 0.6 m*M* DDABr/H_2O systems reveal Newtonian flow behavior within shear rate ($\dot{\gamma}$) range $2–10^3$ s^{-1} where shear viscosity was not different from water viscosity. Similar observations were obtained in the earlier studies[33]. These observations indicate that the size of WM as well as SVs and MLV are not large enough to form entangled networks under quiescent state. The values of δ_{ap} at different contents of CH_3CN in mixed aqueous solvents (Table S1) as well as at different values of $[DDABr]_T$ as shown in Fig. 2 reveal that the polarity of the micellar environment of micellized PSa^- in the presence of WM and SVs mixed with MLV are equivalent to ~25% *v*/*v* CH_3CN and ~50– < 94% *v*/*v* CH_3CN of mixed CH_3CN-H_2O solvent respectively. This conclusion can be used to show that the maximum contribution of $k_M^{mr} K_N K_S[D_n]$, obtained at 0.08 m*M* DDABr, is only nearly 6% compared with k_W^n in Eq. (5) if K_S = 18.6 × 10^3 M^{-1}, k_M ($= k_M^{mr} K_N[Pip]_T$) = 0.0111 s^{-1} (Table S1), $K_N \approx 1$ M^{-1} and $V_M \approx 0.14$ M^{-1} (Ref. 28).

Relatively reliable values of k_M (Table 2) show a decrease with increasing values of [NaBr]. But the value of k_M is similar to the corresponding value of k_M obtained in the presence of spherical/spheroidal micelles (SM) formed from mono chain cationic surfactant CTABr in the ab sence and presence of NaBr[10]. These observations cannot be attributed to possible polarity effect because the values of δ_{ap} remained essentially unchanged for the reactions of Pip with PSa^- in SM, WM, small unilamellar vesicles of CTABr[34], as well as SVs and MLV of DDABr (Fig. 2 and Figs S3 and S4, Supplementary Data). The most plausible cause for these observations may be attributed to different average locations of reactants Pip and PSa^- in SVs mixed with MLV of DDABr[35]. Experimentally determined values of δ_{ap} clearly demonstrate much higher polarity of wormlike micellar environment than that of small vesicular environment of DDABr where DDA^+ bound PSa^-

counterions reside. Although these observations appear to be unusual and interesting, these authors are unable to provide an answer to the question why such observations were found with DDABr/H_2O/NaBr systems but not with CTABr/H_2O and CTABr/H_2O/MX systems where MX represents inert counterionic salts of DDABr and CTABr.

Wagner & coauthors[36] have recently observed spontaneous thermo-reversible formation of DDABr vesicles and WM in a protic ionic liquid. Since the values of δ_{ap} are significantly smaller in the presence of WM than those in the presence of vesicles (Vs), a few kinetic runs were carried out at 0.2 m*M* DDABr, 55 °C and within [NaBr] range 0.0–0.10 *M*. The observed values of δ_{ap} remain unchanged with the change of temperature from 35 to 55 °C. Similar observations were obtained at 0.4 and 0.6 m*M* DDABr. These observations reveal that vesicular structures remain unchanged with the increase in temperature from 35 to 55 °C within $[DDABr]_T$ range 0.2–0.6 m*M*. As a consequence, the vesicular structures are thermally stable under such conditions which could be attributed to probable significantly higher thermodynamic stability of DDABr aggregates in water than that in protic ionic liquid[36].

The calculated values of K_S decreased nonlinearly by nearly 2.5-fold with the increase in [NaBr] from 0–20 m*M*. The values of K_S became almost independent of [NaBr] within its range 20–100 m*M* (Table 1). The values of K_S were found to follow Eq. (1) within [NaBr] range 1.0–20 m*M*, with least-squares calculated values of K_S^0 and $K_{Br/S}$ as (18.0 ± 0.6) × 10^3 M^{-1} and 76 ± 10 M^{-1} respectively. Reliability of the data fit to Eq. (1) is evident from the standard deviations associated with the calculated parameters K_S^0 and $K_{Br/S}$ and from the maximum percent residual error of 6.5 % at 3 m*M* NaBr (Table 1). The calculated value of K_S^0 [= (18.0 ± 0.6) × 0^3 M^{-1}] is similar to the average value of K_S [= (18.7 ± 0.7) × 10^3 M^{-1}] obtained from the duplicate set of kinetic runs at [NaBr] = 0 (Table 1). Nearly 1.8- and 4.2-fold smaller values of K_S^{cald} at 50 and 100 m*M* NaBr respectively (Table 1), reveal a most probable Br^--induced DDABr aggregate structural transition from WM to most likely Vs under such conditions. The values of K_S^0 and $K_{Br/S}$ are expected to be larger in the presence of Vs than WM. The values of K_S, obtained in the presence of vesicular phase, i.e. at > 0.08 m*M* DDABr and [NaBr] range 0.0–10 m*M* were also treated with Eq. (1) and the least-squares calculated values of K_S^0 and $K_{Br/S}$ are (35.0 ± 5.5)×10^3 M^{-1} and 437 ± 141 M^{-1} respectively. The calculated value of K_S^0 is ~ 4 % larger than the average value of K_S (= 33.7×10^3 M^{-1}) obtained experimentally at [NaBr] = 0 (Table 2). Moderately high standard deviations (std) associated with the calculated values of K_S^0 (std = 16%) and $K_{Br/S}$ (std = 32%) reveal that these calculated values are not very reliable.

The value of $K_{Br/S}$ (= 76 M^{-1}) is nearly 3-fold larger in the presence of WM than that (= 25 M^{-1}) in the presence of SM[11] at 35 °C. In view of empirical definition of $K_{Br/S}$, it has been concluded elsewhere that $K_{Br/S} = \Omega_S K_{Br}/K_S$ where Ω_S represents proportionality constant[11,12]. The magnitude of Ω_S is assumed to depend on the molecular characteristics of counterions S^- (the counterion which is expelled by other counterions, such as Br^-, from the cationic micellar pseudophase to the aqueous phase). The magnitude of Ω_S is also assumed to be independent of the molecular characteristics of counterions, such as Br^-, which expel the counterions S^- from cationic micellar pseudophase to the aqueous phase[11]. Thus, $K_{Br/S}^{SM} = \Omega_S^{SM} K_{Br}^{SM}/K_S^{SM}$ and $K_{Br/S}^{WM} = \Omega_S^{WM} K_{Br}^{WM}/K_S^{WM}$ where superscripts represent structures of DDABr/NaBr/H_2O aggregates. Recently, it has been shown that $K_{X/S}^{WM}/K_{Br/S}^{SM} = R_X^{Br} = K_X^{WM}/K_{Br}^{SM}$[11]. Thus, experimentally determined values of $K_{Br/S}^{Vs}$ (= 437 M^{-1}), $K_{Br/S}^{WM}$ (= 76 M^{-1}) and reported value of $K_{Br/S}^{SM}$ (= 25 M^{-1}) give the values of K_{Br}^{Vs}/K_{Br}^{SM} and K_{Br}^{WM}/K_{Br}^{SM} as 17.5 and 3.0, respectively. Studies on counterionic salt-induced cationic micellar growth clearly demonstrate yet qualitatively that the increase in the counterion binding efficiency to cationic surfactant aggregates enhances the aggregate structural transitions from SM-to-WM-to-Vs[11]. In view of these studies, the calculated values of K_{Br}^{Vs}/K_{Br}^{SM} (= 17.5), K_{Br}^{WM}/K_{Br}^{SM} (= 3.0), K_S^{0SM} (= 7.0 × 10^3 M^{-1}), K_S^{0WM} (= 18.7 × 10^3 M^{-1}) and K_S^{0Vs} (= 33.7 × 10^3 M^{-1}) appear to be plausible. It may be relevant to mention that the value of conventional ion-exchange constant, $K_X^{Br} (= K_X^{WM}/K_{Br}^{WM})$ for X = monoanionic salicylate ion for ion-exchange process occurring at the surface of CTABr WM is 20 (Ref. 30). The reported value of $R_X^{Br} (= K_X^{WM}/K_{Br}^{SM})$ for X = dianionic salicylate ion is 44 (Ref. 44). These results show that K_{Br}^{WM}/K_{Br}^{SM} = 2.2, which may be compared with the value (= 3.0)

obtained in the present study where double-tail cationic surfactant (DDABr) is different from mono-tail cationic surfactant CTABr. Unpublished observations reveal that the values of R_X^{Br} are nearly same for X representing mono- and dianionic 4-methoxysalicylate. The probable answer to the question on how counterion affinity to ionic aggregates affects the structure of aggregates of aqueous ionic surfactants is recently explained qualitatively elsewhere[34].

Analysis of kobs versus [NaBr] at a constant [DDABr]T

Recently, the nonlinear increase in k_{obs} with the increase of [MX] (MX = 2,3- and 3,5-$Cl_2C_6H_3CO_2Na$) at a constant concentration of CTABr micelles/ nanoparticles, obtained for piperidinolyss of PSa^- has been attributed to CTABr/MX/H_2O nanoparticles catalysis[39]. Similarly, the values of k_{obs} increase nonlinearly with increase of [NaBr] at a constant $[DDABr]_T$ as exhibited by Fig. 5 may be attributed to DDABr/NaBr/H_2O nanoparticles/micelles catalysis. This conclusion is drawn for the reason that the values of k_{obs} (= k_W) are independent of [NaBr] within its range 0.0–0.10 *M*, in the absence of DDABr micelles/ nanoparticles (Table 1 and Fig. 5). Figure 5 represents plots of k_{obs} versus [NaBr] at some different representative values of $[DDABr]_T$. The experimental data (k_{obs} versus [NaBr]) shown in Fig. 5 were treated with empirical equation, Eq. (7),

$$k_{obs} = \frac{k_0 + k_{Br}[NaBr]}{1 + K^{Br/S}[NaBr]} \quad \ldots(7)$$

where $k_0 = k_{obs}$ at [NaX] = 0, k_{Br} and $K^{Br/S}$ are empirical constants. The empirical constant k_{Br} represents apparent DDABr/NaX/H_2O nanoparticles catalytic constant. The nonlinear least-squares calculated values of empirical constants, k_{Br} and $K^{Br/S}$, at 0.07, 0.10, 0.20, 0.30 and 0.40 m*M* DDABr are summarized in Table 3. These observed data were also treated with Eq. (2) and the nonlinear least-squares calculated values of θ and $K^{Br/S}$ are also summarized in Table 3. The least-squares calculated values of k_{cald} (pseudo-first-order rate constant), calculated from Eq. (2) with the value of θ and $K^{Br/S}$ listed in Table 3, remain unchanged with the corresponding values of k_{cald} calculated from Eq. (7) with the values of k_{Br} and $K^{Br/S}$ listed in Table 3. This analysis shows that $k_{Br} = \theta K^{Br/S}$ and the value of $K^{Br/S}$ remains unchanged with the change of equation (for the determination of $K^{Br/S}$) from Eq. (2) to Eq. (7). It has been described elsewhere[11] that empirical constants, θ and $K^{Br/S}$, of Eq. (2), may be expressed by Eqs (8) and (9) respectively.

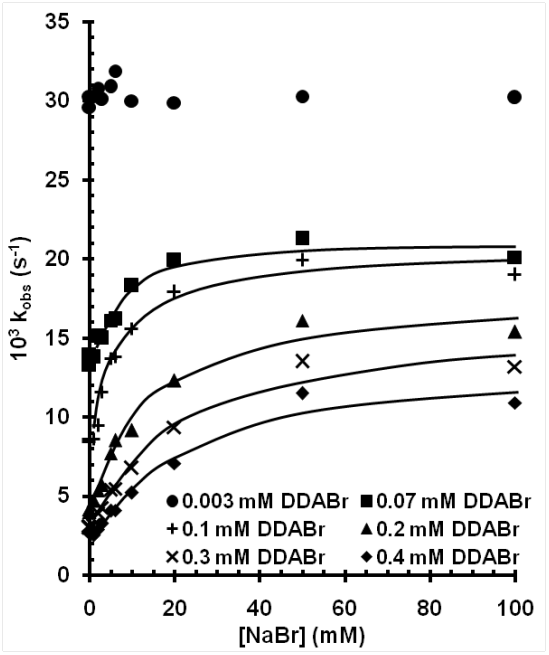

Fig. 5 — Plots showing the dependence of k_{obs} upon [NaBr] for piperidinolysis of PSa^- at 0.2 m*M* PSa^-, 0.1 *M* Pip, 0.03 *M* NaOH, 35 °C and different constant values of $[DDABr]_T$. [The solid lines are drawn through the calculated data points using Eq. (2) with kinetic parameters (θ or k_{Br} and $K^{Br/S}$), listed in Table 3, at $[NaBr]_0^{op}$(m*M*) = 1.0 (■), 0.6 (+), 0.7 (▲), 1.0 (×) and 1.9 (◆)].

Table 3 — Values of kinetic parameters, k_{Br}, θ and $K^{Br/S}$, calculated from Eq.s (2) and (7)[a]

$[D]_T$ (m*M*)	$[NaBr]_0^{op}$ (m*M*)	$10^3 k_0$[b] (s^{-1})	$10^3 k_{Br}$ ($M^{-1}s^{-1}$)	$K^{Br/S}$ (M^{-1})	$10^3\theta$ (s^{-1})	$F_{Br/S}$[c]	μ[d] (M^{-1})	$10^{-3} K_S^0$ (M^{-1})	Structure of nanoparticles
0.07	1.0	13.6 ± 0.3[e]	2926 ± 683[f]	136 ± 34[f]	21.6 ± 0.6[f]	0.70	215	18.7	WM
0.10	0.6	8.52 ± 0.11	3003 ± 423	145 ± 24	20.7 ± 0.6	0.67	352	33.7	Vs
0.20	0.7	4.09 ± 0.09	1392 ± 180	78.4 ± 12.7	17.8 ± 0.8	0.58	340	33.7	Vs
0.30	1.0	3.07 ± 0.08	825 ± 117	51.4 ± 9.6	16.1 ± 0.9	0.54	269	33.7	Vs
0.40	1.9	2.70 ± 0.02	580 ± 126	41.9 ± 12.2	13.9 ± 1.2	0.45	215	33.7	Vs

[a][PSaH] = 0.2 m*M*, 30 m*M* NaOH, 100 m*M* Pip, 35°C, λ = 370 nm, aqueous reaction mixture for each kinetic run contains 2 %*v/v* CH_3CN and D = DDABr.
[b]Average value, obtained from duplicate kinetic runs carried out at [NaBr] = 0.
[c]$F_{Br/S} = \theta/k_W$ with $10^3 k_W = 30.9 \pm 0.2\ s^{-1}$. [d]$\mu = k_{Br}/k_0$.
[e]Error limits are average deviations. [f]Error limits are standard deviations.

$$\theta = F_{Br/S} k_W^{NaBr} \quad \ldots (8)$$

where $k_W^{NaBr} = k_{obs}$ at a typical value of [NaBr] as well as $[DDABr]_T = 0$, and $F_{Br/S}$ is an empirical constant[10,28] whose magnitude should (by definition) vary from > 0 to ≤ 1.0, and

$$K^{Br/S} = K_{Br/S}/(1 + K_S^0[D_n]) \quad \ldots (9)$$

where $K_S^0 = K_S$ at [NaBr] = 0 and $[D_n] = [DDABr]_T$ – CMC or CVC.

The values of k_{obs} were found to be independent of [NaBr] within its range 0.00–0.10 *M* at 0.003, 0.02 and 0.04 m*M* DDABr. The mean value of $k_{obs} (= k_{obs}^{av})$ are similar to the corresponding values of k_{obs} (= k_W) at [NaBr] = 0. The values of the ratio $k_W/k_0 (\approx k_W/k_{obs}^{av})$ are 1.01, 1.19 and 1.44 at 0.003, 0.02 and 0.04 m*M* DDABr, respectively. These observations do not favour the probable cause, such as salt effect, for the nonlinear increase in k_{obs} with the increase in [NaBr] (Fig. 5) at $[DDABr]_T \geq 0.07$ m*M*. The value of k_W/k_0 of 1.01 reveals that DDABr micelles do not exist at 0.003 m*M* DDABr and within [NaBr] range 0.0–0.10 *M*. The values of k_W/k_0 of >1.0 indicate that DDABr micelles exist at 0.02 and 0.04 m*M* DDABr and within [NaBr] range 0.0–0.10 *M*. But under such typical conditions $k_0 \approx \theta$ in Eq. (2).

The decrease in the values of $K^{Br/S}$ with increasing $[DDABr]_T$ at a constant structural aspect of DDABr/NaBr/H_2O nanoparticles (Table 3) is expected in view of Eq. (9). Apparent DDABr/NaBr/H_2O nanoparticle catalytic efficiency or rate enhancement (μ) for piperidinolysis of PSa^- may be expressed by the relationship: $\mu = k_{Br}/k_0$ where $k_0 = k_{obs}$ at [NaBr] = 0 and at a constant $[DDABr]_T$ >> CMC or CVC. Such calculated values of μ at 0.07 m*M* DDABr (in the presence of wormlike micelles, WM) and 0.1, 0.2, 0.3 and 0.4 m*M* DDABr (in the presence of vesicles, Vs) are summarized in Table 3. The values of k_{Br} decrease from 3.00 to 0.58 M^{-1} with the increase in $[DDABr]_T$ from 0.10 to 0.40 m*M* in the presence of vesicles (Vs). These observations may be attributed to the relationship: $k_{Br} = \theta K^{Br/S}$ and in view of Eq. (9), the value of $K^{Br/S}$ should decrease with the increase in $[D_n]$. Significantly large values of k_{Br} may be ascribed to: (i) the ability of non-reactive counterions Br^- to expel the reactive counterions, PSa^-, from the micro-reaction environment of the nanoparticles to the bulk water phase and (ii) more than 10- fold larger value of the second-order rate constants for the nucleophilic reaction of Pip with PSa^- in bulk water phase than in the less polar microreaction environment of DDABr/NaBr/H_2O nanoparticles.

Conclusions

In summary, the kinetic data provide experimental evidence for the presence of both CMC and CVC in the DDABr micelles-catalyzed piperidinolysis of PSa^-. The values of DDABr micellar binding constant (K_S) of PSa^- are 18.7×10^3 and 33.7×10^3 M^{-1} in the presence of WM and Vs respectively, while the value of CTABr micellar binding constant of PSa^- is 7.0×10^3 M^{-1} in the presence of SM. The estimated values of K_{Br}^{Vs}/K_{Br}^{SM} and K_{Br}^{WM}/K_{Br}^{SM} are 17.5 and 3.0 respectively. The polarity of the micellar environment of micellized PSa^- (i.e. PSa^-_M) in the presence of WM, and SVs mixed with MLV are equivalent to ~24 and 50 to 92% *v/v* CH_3CN of mixed CH_3CN–H_2O solvent respectively. These observations are distinctly different from those obtained in the presence of CTABr micelles where the polarity of micellar environment of PSa^-_M has been found to be equivalent to ~90–92% *v/v* CH_3CN of mixed CH_3CN–H_2O solvent and this polarity remains unchanged with the change in the micellar structure from SM-to-WM-to-small unilamellar vesicles [34]. The values of $K_{Br/S}$ or $K_{X/S}$, at a constant temperature, may be used as the indicator for the presence of SM or WM or Vs in an aqueous solution containing CTABr aggregates.

Supplementary Data

Supplementary data associated with this article are available in the electronic form at http://www.niscair.res.in/jinfo/ijca/IJCA_56A(11)1132-1142_SupplData.pdf.

Acknowledgement

This research is supported by UM High Impact Research Grant UM–MOHE UM.C/625/1/HIR/MOHE/ SC/07 from the Ministry of Higher Education, Malaysia.

References

1 Cordes E H, *Pure Appl Chem*, 50 (1978) 617.
2 Burma N J, Serana P M, Blandamer J B & Engberts F N, *J Org Chem*, 69 (2004) 3899.
3 Munoz M, Rodriguez A, Graciani M D & Moya M L, *Int J Chem Kinet*, 34 (2002) 445.
4 Brinchi L, Germani R, Goracci L, Savelli G & Bunton C A, *Langmuir*, 18 (2002) 7821.
5 Buwalda R T, Stuart M C A & Engberts J B F N, *Langmuir*, 16 (2000) 6780.

6 Renoncourt A, Vlachy N, Bauduin P, Drechsler M, Touraud D, Verbavatz J-M, Dubois M, Kunz W & Ninham B W, *Langmuir*, 23 (2007) 2376.
7 Shukla A & Rehage H, *Langmuir*, 24 (2008) 8507.
8 Vera S & Rodenas E, *J Phys Chem*, 90 (1986) 3414.
9 Zakharova L, Valeeva F, Zakharov A, Ibragimova A, Kudryavtseva L & Harlampidi H, *J Colloid Interface Sci*, 263 (2003) 597.
10 Khan M N, Arifin Z, Ismail E & Ali S F.M, *J Org Chem*, 65 (2000) 1331.
11 Khan M N, *Adv Colloid Interface Sci*, 159 (2010) 160.
12 Yusof N S M & Khan M N, *Langmuir*, 26 (2010) 10627 and references cited therein.
13 Rodriguez A, Del Mar Graciani M, Cordobes F & Moya M L, *J Phys Chem B*, 113 (2009) 7767.
14 Thalody B & Warr G G, *J Colloid Interface Sci*, 188 (1997) 305.
15 Magid L J, Han Z, War G G, Cassidy M A, Butler P W & Hamilton W A, *J Phys Chem. B*, 101 (1997) 7917.
16 Menger F M & Williams D Y, Underwood A L, Anacker E W, *J Colloid Interface Sci*, 90 (1982) 546.
17 Jungwirth P & Tobias D J, *Chem Rev*, 106 (2006) 1259.
18 Grillo I, Penfold J, Tucker I & Cousin F, *Langmuir*, 25 (2009) 3932 and references cited therein.
19 Ono Y, Kawasaki H, Annaka M & Maeda H, *J Colloid Interface Sci*, 287 (2005) 685.
20 Kaur R, Kumar S & Aswal V K, *Colloid Polym Sci*, 290 (2012) 127.
21 Marques E F, Regev O, Khan A, Miguel Maria da G & Lindman B, *J Phys Chem B*, 103 (1999) 8353.
22 Junquera E, Arranz R & Aicarf E, *Langmuir*, 20 (2004) 6619.
23 Brinchi L, Di Profio P, Geramani R, Goracci L, Savelli G, Gilliff N D & Bunton C A, *Langmuir*, 23 (2007) 436.
24 Kunitake T, Okahata Y, Ando R, Shinkai S & Hirakawa S, *J Am Chem Soc*, 102 (1980) 7877.
25 Yusof N S M, Razak N A & Khan M N, *J Oleo Sci*, 62 (2013) 257.
26 Scarpa M V, Araujo P S, Schreier S, Sesso A, Oliveira A G, Chaimovich H & Cuccovia I M, *Langmuir*, 16 (2000) 993.
27 Brinchi L, Germani R, Braccalenti E, Spreti N, Tiecco M & Savelli G, *J Colloid Interface Sci*, 348 (2010) 137.
28 Khan M N, Ariffin Z, Lasidek M N, Hanifiah M A M & Alex G, *Langmuir*, 13 (1997) 3959 and references cited therein.
29 Bunton C A, in *Surfactant in Solutions*, edited by K L Mittal & D O Shah, (Plenum, New York) 1991.
30 Bunton C A & Savelli G, *Adv Phys Org Chem*, 22 (1987) 213.
31 Broxton T J, Christie J R & Chung R P T, *J Org Chem*, 53 (1988) 3081.
32 Marques E F, Regev O, Khan A & Lindman B, *Adv Colloid Interface Sci*, 100-102 (2003) 83.
33 Soltero J F A, Bautista F, Pecina E, Puig J E, Manero O, Proverbio Z & Schulz P C, *Colloid Polym Sci*, 278 (2000) 37 and references cited therein.
34 Yusof N S M & Khan M N, *J Phys Chem B*, 116 (2012) 2065.
35 Otto S, Engberts J B F N & Kwak C T, *J Am Chem Soc*, 120 (1998) 9517.
36 Lopez-Barron C R, Li D, De Rita L, Basavaraj M G & Wagner N J, *J Am Chem Soc*, 134 (2012) 20728.
37 Bachofer S J & Simonis U, *Langmuir*, 12 (1996) 1744.
38 Khan M N, Ismail E & Yusof N S M, *Colloids Surf A*, 361 (2010) 150.
39 Razak N A, Yusof N S M & Khan M N, *J Taiwan Inst Chem Engineers*, 45 (2014) 2777.